J Comput Aided Mol Des (2008) 22:553–561
DOI 10.1007/s10822-008-9198-3

Modeling dimerizations of transmembrane proteins using Brownian dynamics simulations

Meng Cui · Mihaly Mezei · Roman Osman

Received: 12 December 2007 / Accepted: 7 February 2008 / Published online: 13 March 2008

Abstract The dimerizations of membrane proteins, Outer Membrane Phospholipase A (OMPLA) and glycophorin A (GPA), have been simulated by an adapted Brownian Dynamics program. To mimic the membrane protein environment, we introduced a hybrid electrostatic potential map of membrane and water for electrostatic interaction calculations. We added a van der Waals potential term to the force field of the current version of the BD program to simulate the short-range interactions of the two monomers. We reduced the BD sampling space from three dimensions to two dimensions to improve the efficiency of BD simulations for membrane proteins. The OMPLA and GPA dimers predicted by our 2D-BD simulation and structural refinement is in good agreement with the experimental structures. The adapted 2D-BD method could be used for prediction of dimerization of other membrane proteins, such as G protein-coupled receptors, to help better understanding of the structures and functions of membrane proteins.

Keywords Molecular modeling · Brownian dynamics · Molecular recognition · Transmembrane protein · Dimerization

M. Cui (✉) · M. Mezei · R. Osman (✉)
Department of Structural and Chemical Biology, Mount Sinai School of Medicine, New York University, Box 1218, New York, NY 10029, USA
e-mail: meng.cui@mssm.edu; meng.mcui@gmail.com

R. Osman
e-mail: roman.osman@mssm.edu

Introduction

wDimerization is essential for the function of many membrane proteins, including protein-tyrosine kinase receptors, cytokine receptors, antigen receptors, tumor necrosis receptors, protein-serine/threonine kinase receptors, and G protein-coupled receptors (GPCRs) [1–6]. Growing experimental evidence suggests that GPCRs function as dimers (or higher oligomers), and that dimerization can occur among identical GPCRs (homodimers) as well as among close but distinct family members (heterodimers). Dimerization of GPCRs affects ligand binding, receptor activation, desensitization and trafficking, as well as receptor signaling [7, 8].

To better understand the relation between dimerization and the biological function of transmembrane proteins, a detailed structural model would be very important. Both experimental and computational approaches have contributed to the current view of GPCR dimerization. Experimental approaches, such as Western blot analysis, coimmunoprecipitation, fluorescence resonance energy transfer (FRET) and bioluminescence resonance energy transfer (BRET), provided convincing evidence that dimerization takes place but it is difficult to construct a detailed structural model on the basis of these results [4, 9–16]. The projection structures of invertebrate and vertebrate rhodopsins obtained by cryo-electron microscopy of two-dimensional crystals provided valuable information of the alignment of rhodopsins in vivo [17–19]. Recently, the organization of rhodopsin in native membranes was determined by atomic force microscopy (AFM) [12, 14], which demonstrated that the structural dimers of rhodopsin are organized in paracrystalline arrays. Even though the AFM experiments did not reach atomic level resolution, a molecular model was developed based on the results, and a detailed structure of the rhodopsin dimer was

proposed [13]. More recently, the homodimer interface in dopamine D2 receptors has been mapped by crosslinking of substituted cysteines, and it has been demonstrated that the changes at the transmembrane homodimer interface determine the activation of GPCRs [20].

An alternative approach is to use de novo computational approaches to construct molecular models of the dimers. Computational approaches can be based on bioinformatics or molecular docking methods. Bioinformatics methods, based on sequence and genomic information, can predict probable regions involved in dimerization of proteins [21]. For example, a new subtractive correlated mutation method has been developed by Filizola et al. [22, 23], and its application to opioid receptor homo/hetero-dimers prediction showed that opiod receptors could dimerize in several patterns. Docking approaches depend on the availability of a three-dimensional structure for the monomer(s) and some information of potential interaction surfaces to predict protein–protein interactions [24]. However, most of the current docking programs need to be extended to be able to simulate dimerization of membrane proteins in a hybrid of a water/membrane environment. In addition, most of the docking programs sample the entire three-dimensional (3D) space, which seems to be computationally wasteful for docking in the nearly planar environment of the membrane. The constraint imposed on the monomers by localizing them to the membrane allows the reduction of sampling space from 3D to 2D with a concomitant increase in the efficiency of docking simulations of membrane protein dimerization.

The docking feature of the Brownian Dynamics (BD) approach has been used in the past to predict protein–protein interactions [25–27]. In earlier work we used BD to successfully simulate the recognition between scorpion toxins and potassium channels. The results indicate that the strong electrostatic interactions between scorpion toxins and potassium channels are the main driving force for the recognition and association [28–31]. However, since the current BD approach considers electrostatic forces as the biasing guide in the otherwise Brownian stochastic motions, it may not be suitable to predict protein complexes in which electrostatic interactions between proteins are not dominant. In membrane proteins electrostatic interactions are clearly not dominant as illustrated in the recent study of the dimerization of the D2 receptor [20].

Here we describe an attempt to adapt the conventional BD approach to the prediction of membrane protein dimerization. To this end we have modified several aspects of the computational protocol. We have modified the calculation of the electrostatic potential to account for the different dielectric properties of the water/membrane environments. Since electrostatics plays a substantially smaller role in membrane protein dimerization, we have added a van der Waals term to the current BD energy expression and its force field. Finally, to take advantage of the spatial limitation imposed by the membrane we have reduced the BD sampling space from 3D to 2D.

The adapted BD program has been used to predict the dimerizations of OMPLA and GPA. The crystal structure of OMPLA and Nuclear Magnetic Resonance (NMR) structures of GPA are available, thus allowing us to test our predictions based on this computational approach. The consistency of predicted dimers of OMPLA, and GPA with the experimental structures indicates that the modified BD approach could be used for predicting dimerization of other membrane proteins, such as GPCRs.

Materials and methods

Atomic coordinates

The atomic coordinates of the OMPLA dimer at a resolution of 2.1 Å were obtained from the Protein Data Bank (PDB) [32], entry 1QD6 [33]. The residues missing in the crystal structure (26–29) were generated by the MODLOOP server (http://alto.compbio.ucsf.edu/modloop/) [34, 35]. Each OMPLA monomer consists of a 12-stranded antiparallel β-barrel with a flat side that is the dimerization interface and a convex side that faces the lipid membrane. The 12 amphipathic β-strands traverse the membrane, forming a hydrophobic outer surface flanked by rings of aromatic residues at the area of the polar head-groups that presumably coincide with the boundaries of the membrane bilayer. Dimerization occurs almost exclusively between the apolar membrane-embedded parts, and results in the formation of substrate-binding pockets and functional oxyanion holes, which are catalytically important but are absent in monomeric OMPLA [33].

The atomic coordinates of the GPA dimers were obtained form PDB, entry 1AFO [36]. The dimeric structures of GPA peptide (residues 62–101) were determined by heteronuclear nuclear magnetic resonance (NMR) methods, and there are 20 NMR structures in 1AFO. The residues 71–95 of GPA were used for this study. Each NMR structure of GPA peptide (residue 71–95) was optimized by using the implicit membrane Generalized Born (GB) model in CHARMM program. The dimeric structure with the lowest interaction energy between two monomers was selected for BD docking studies.

BD simulations

The program package MacroDox, version 3.2.2 [37], was used to assign charges on proteins, solve the linearized Poisson–Boltzmann equation, and run the BD simulations.

The BD algorithm for this program has been detailed by Northrup et al. [38, 39].

BD simulations of the two interacting macromolecules in a solvent is approximated by a series of small displacements chosen from a distribution that is equivalent to the short time solution of the Smoluchowski diffusion equation [40] in the presence of external forces. The basic Ermak–McCammon algorithm [41] is employed to simulate the translational Brownian motion of two interacting proteins as the displacements $\Delta\mathbf{r}$ of the relative separation vector $\mathbf{r}$ between the centroids of the two proteins in a time step Δt according to the relation

$$\Delta\mathbf{r} = \frac{D \cdot \Delta t}{k_B T} \cdot \mathbf{F} + \mathbf{S} \tag{1}$$

where D is the translational diffusion coefficient for the relative motion and is assumed to be isotropic; $\mathbf{F}$ is the systematic inter-particle force, which is computed during Brownian dynamics; k_B is the Boltzmann constant and T the absolute temperature; $\mathbf{S}$ is the stochastic component of the displacement arising from collisions of proteins with solvent molecules, which obeys the relationship

$$\langle S^2 \rangle = 2D\Delta t \tag{2a}$$

$$\langle S \rangle = 0 \tag{2b}$$

A similar equation governs the independent rotational Brownian motion of each particle, in which the force is replaced by a torque and D is replaced by an isotropic rotational diffusion coefficient D_{ir} for each particle i.

In the original approach, only long-range electrostatic interactions, and van der Waals excluded volumes are used. In the adapted approach $\mathbf{F}$ includes in addition to the electrostatic also the repulsive and attractive van der Waals.

Because the residues of OMPLA and GPA are partly in water and partly in membrane, the electrostatic potential was calculated in a hybrid environment with dielectric constants of 2 and 78 assigned to mimic the membrane and water environments, respectively. The dielectric constant of the protein was set to 4. The CHARMm22 force field was used to assign the atomic charges for OMPLA and GPA. After charge assignments, the electrostatic potentials of OMPLA and GPA were computed with the linearized Poisson–Boltzmann equation,

$$-\nabla\varepsilon(r)\nabla\phi(r) + \varepsilon(r)\kappa^2\phi(r) = \rho(r)\varepsilon_0 \tag{3}$$

where $\varepsilon(r)$ is the dielectric constant, $\phi(r)$ is the electrostatic potential, and $\rho(r)$ is the charge density, all at position r; κ is the inverse Debye length. The assignment of $\varepsilon(r)$ to the membrane and water was done on the basis of identifying the membrane surface as described in "Results and discussion". The Poisson–Boltzmann equation was solved by the method of Warwicker and Watson [42] as implemented in the MacroDox program. The electrostatic potentials were determined on 131 × 131 × 131 cubic grids centered on the center of mass of Monomer I. The resolutions of the inner and outer grids for OMPLA and GPA were 1.2 and 3.6 Å, respectively.

Next, modified BD simulations of the dimerization of OMPLA and GPA were performed to identify the favorable complex(es). For simulations of protein–protein interactions in which the proteins are treated as rigid bodies, there are only two solute particles. Without loss of generality one of the proteins (Monomer I) is positioned at the origin and the translational and rotational motions are simulated for the other protein (Monomer II) [43] (See Fig. 1). We reduced the dimensionality of BD sampling from three dimensions to two dimensions with the relaxations of motions perpendicular to the membrane (±1 Å for OMPLA and GPA) and rotations out of the membrane (±15° for OMPLA and ±45° for GPA), as a suitable approximation for simulations of membrane proteins that translate and rotate within the two-dimensional membrane.

Trajectories were started with Monomer II at a random position and orientation on the b-cylinder with radius b (50 Å and 30 Å for OMPLA and GPA, respectively) (Fig. 1). Monomer II was subjected to four forces: electrostatic, van der Waals, the random Brownian force, and the frictional force due to solvent viscosity. All the coordinates and interaction energies were recorded when the distances between the monomers were smaller than 35 Å for OMPLA or 15 Å for GPA during the simulations. The

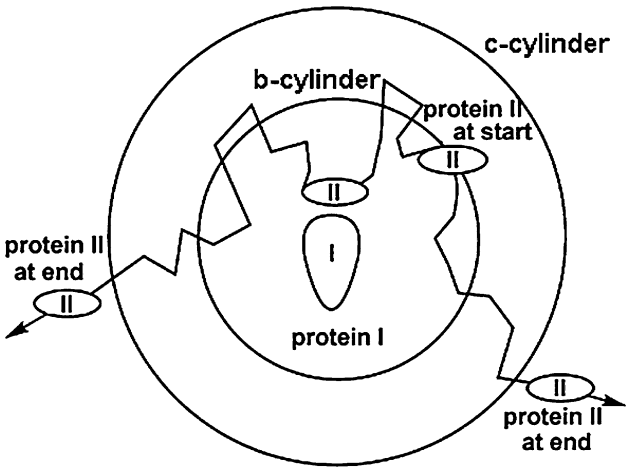

Fig. 1 A systematic representation of the Brownian dynamics simulation of the association between two proteins. Simulations are conducted in coordinates defined relative to the position of the center of the protein, protein I. At the beginning of each trajectory the second mobile protein, protein II, is positioned with a randomly chosen orientation at a randomly chosen point on the inner cylinder of radius b. BD simulation is then performed until this protein diffuses outside the outer cylinder of radius q. During the simulation, the complex(es) satisfying the reaction criteria for encounter complex formation is recorded

trajectory was terminated when monomer II escaped the q-cylinder (65 Å for OMPLA and 45 Å for GPA) or was taken longer than 20 ns. We ran 3,000 BD simulations for OMPLA and 50,000 BD simulations for GPA at a temperature of 298.15 K. The recorded structures in each trajectory were ranked based on the interaction energies between two monomers. Only the most favorable recorded structures from each trajectory were selected, and ranked based on the interaction energies. The dimeric structures of OMPLA and GPA with favorable interaction energies were selected for the local energy minimization and cluster analysis.

Structure refinements by local minimization

The structures of the OMPLA and GPA dimer obtained by BD simulations was subjected to energy refinement using a newly developed rigid-body energy minimization program based on the downhill simplex method [44] which uses the same force field as the BD simulations in our work. Six variables (three translation values and three rotation values of monomer II relative to monomer I) were allowed to change for the minimization.

Results and discussion

Adapted BD method for membrane proteins

BD sampling space reduction

In simulations of the dimerization of membrane proteins, it is more efficient to sample the two-dimensional space. To that end, we adapted the MacroDox 3.2.2 program, and restricted the motions in the BD simulations to displacements within a two dimensional space. The 2D-BD simulations require knowing the relative orientation and the relative position along z-direction between two proteins before the simulations. However, this information is not available without knowing the complex structure, which makes the prediction impossible. So it is necessary to introduce the out-plane relaxations to 2D-BD method for the most cases. We have included the motions in the z-direction and the out-plane rotations of monomer II. Thus, the usual b-sphere and q-sphere of 3D-BD simulations were replaced with the equivalent b- and q-cylinders (see "Materials and methods"). In this work, we allowed the motions in z-direction within ± 1 Å for both OMPLA and GPA, and the out-plane rotations within $\pm 15°$ for OMPLA and $\pm 45°$ for GPA. The values we chosen here are based on the crystal structure of OMPLA dimer (0 Å and 0°) and NMR structures of GPA dimers (0 Å and $\sim 40°$). These values depend on the system to be studied. However, increasing these values will increase the sampling space dramatically.

Hybrid membrane/water electrostatic potential

It is essential to treat the electrostatic force correctly for the BD simulations, since it provides long-range guidance of the motion of proteins. We have adapted the program to solve PB equation for hybrid membrane/water environment defining the local dielectric properties $\varepsilon(r)$ according to the boundaries of the membrane and the protein. To build the hybrid water/membrane environment for electrostatic potential calculations, and to perform the BD docking simulations, it is also important to define the water/membrane interface for the proteins within the membrane. The dielectric constant varies by a factor of ~ 40 between membrane ($\varepsilon = 2$) and water ($\varepsilon = 78$) environments.

We determined the interface of membrane/water of OMPLA by locating the positions of Trp. Statistical analyses of membrane proteins show that Trp has a preference for the interfacial membrane–water environment [45, 46]. The chemical properties of the indole side chain of Trp appear ideally suited for interacting with the phospholipids head groups, which defines the polar–apolar interface [47]. Here we used Trp as the reference residues to determine the membrane–water interface. There are 16 Trp residues in the OMPLA dimer, of which 10 (Trp 97, Trp98, Trp155, Trp176 and Trp 216 for each monomer) are located in upper part, and six (Trp78, Trp 131 and Trp 169 for each monomer) in the lower part of the protein. To approximate the plane of the membrane, we calculated the center of masses (COMs) of Cα atoms of Trp residues for the upper and lower parts, respectively, and translated, as a rigid body, the lower part Cα atoms of Trp residues to the upper part along the COMs direction (this is equivalent to superimposing the two COMs). The largest root-mean-square deviation (RMSD) from the plane fitted to the Cα atoms of all the Trp residues was 2.9 Å. After removing the Cα atoms of Trp 131, Trp 176 and Trp 216 with large RMSD values, the deviation from the newly fitted plane was <0.7 Å. The distance from the upper to the lower level is about 24 Å. We oriented the OMPLA dimer protein along the normal direction of the fitted plane, which was defined as the z-direction for 2D-BD simulations.

GPA peptide (residue 71–95), which is an α helix, was oriented to parallel the normal direction of membrane plane. The upper and lower membrane planes are defined as ± 14.5 Å from the center of mass of GPA peptide.

Including the van der Waals potential

For docking simulations, it is critical to include the short-range interaction energy terms between the

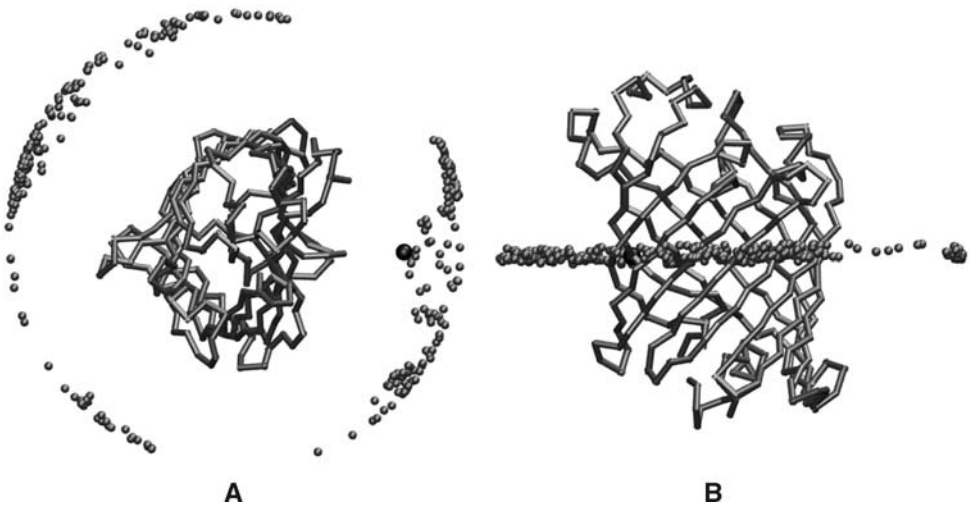

Fig. 2 The center of mass distribution of Monomer II around Monomer I of OMPLA from adapted 2D-BD simulations (**a**: top view; **b**: side view)

proteins. In the current version of BD programs, however, usually only long-range electrostatics interaction energy term is included. So we adapted the force field of the MacroDox program by adding additional van der Waals energy term. We used a smoothed 12-6 Lennard–Jones potential to model the van der Waals energy term, and the 12-6 parameters were converted from AMBER parameters [48]. Four united atom types (C, N, O, S) van der Waals potential maps of Monomer I were calculated before BD simulations. We used the same cubic grid dimensions (131 × 131 × 131) and grid resolutions of 1.2 Å centered on the center of mass of Monomer I for van der Waals potential maps. However, unlike for the electrostatics potential map, only the inner grid maps of van der Waals potentials are calculated due to the nature of short-range interactions.

Applications of adapted 2D-BD simulations

To validate the adapted 2D-BD method, we applied it to simulate the dimerization of transmembrane proteins OMPLA and GPA, whose experimental structures are available for comparison.

BD simulations of the dimerization of OMPLA

In 837 instances out of a total of 3,000 independent BD trajectories of OMPLA, the critical distance criterion (35 Å) was met. The interaction energies between the monomers in each trajectory with recorded structures were ranked, and the complex with the lowest interaction energy was selected in each trajectory. About 782 complexes (Fig. 2) with negative interaction energies were obtained

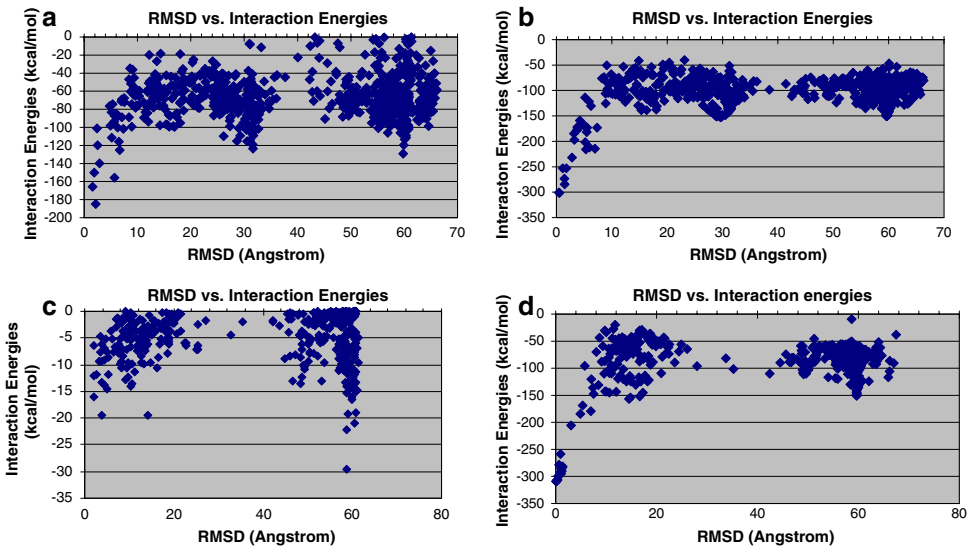

Fig. 3 Interaction energies of predicted dimer complexes vs. RMSD between the predicted and crystal structure of OMPLA Monomer II. (**a**) BD simulations with vdw terms; (**b**) BD simulations with vdw terms followed by local energy minimizations; (**c**) BD simulations without vdw terms; (**d**) BD simulations without vdw terms followed by local energy minimizations

for the following local minimization and statistical cluster analysis.

We used the downhill simplex method with the same force field as in the BD simulations to optimize the local configurations of all the dimer structures of OMPLA with the negative interaction energies. To evaluate the BD-predicted OMPLA dimer, we calculated the root-mean-square deviation (RMSD) of α carbon atoms between the predicted and crystal structures of monomer II, and generated the plots of interaction energies vs. RMSD (Fig. 3a, b present the results before and after local energy minimization, respectively). From Fig. 3, one can see that the dimer complex structures with lower interaction energies have smaller RMSDs to the native structure, which means that one can distinguish the native structure from non-native ones by comparing the interaction energies. The local energy minimization significantly improves the predictions.

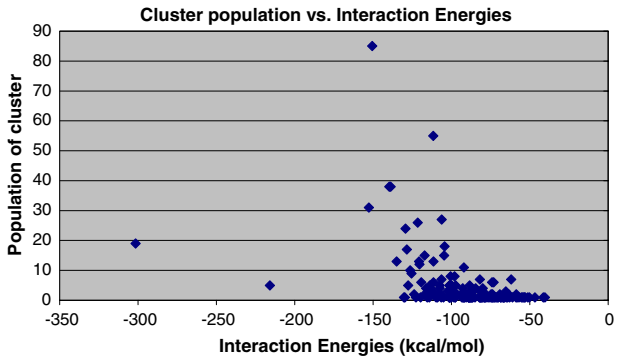

Fig. 4 Cluster population vs. lowest interaction energies between Monomers I and II of OMPLA in the cluster (3.5 Å cutoff based on all the α carbon atoms of Monomer II)

In order to explore importance of the contributions of vdw terms to the BD simulations, we turned off the terms during the simulations. About 408 complexes with negative interaction energies were obtained from the simulations. The plot of interaction energies vs. RMSD (Fig. 3c) shows no correlations between RMSD and interaction energy, which means that one cannot identify the native structure from the simulations without vdw terms by using the lowest interaction energies. However, after we performed additional local energy minimizations with the vdw terms on these complexes, the correlations of interaction energies and RMSD were recovered (Fig. 3d).

A statistical cluster analysis for 782 optimized complex structures from the BD simulations with vdw terms based on 3.5 Å cutoff for all the α carbon atoms, produced 163 clusters. The clustering algorithm used picks the element that has the largest number of conformation within the cutoff and makes it a cluster. This cluster is then removed and the procedure is repeated until no more configurations are left. The plot of cluster population vs. lowest interaction energies of the cluster is shown in Fig. 4. From Fig. 4, one can see that the cluster with the lowest interaction energy is more stable than the rest of clusters. The predicted structure with lowest interaction energy superimposed on the crystal structure is shown in Fig. 5. The BD predicted structure is very close to the crystal structure (RMSD = 0.52 Å) of OMPLA, which indicates success of the prediction.

BD simulations of the dimerization of GPA

In 22,246 instances out of a total 50,000 independent BD trajectories of GPA, the critical distance (15 Å) was met. We

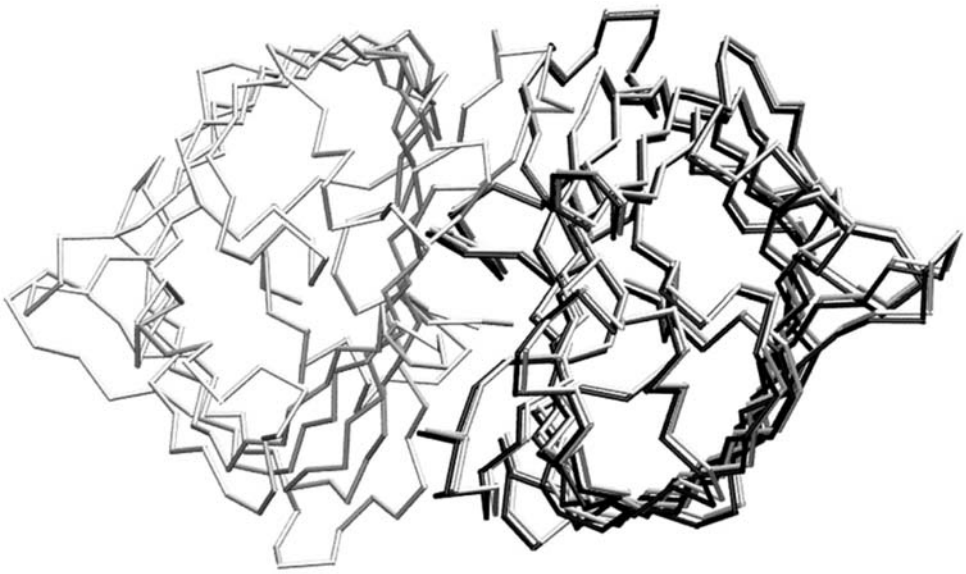

Fig. 5 Comparison of crystal structure and 2D-BD predicted structures. The BD-predicted Monomer II (right, in black) is very close to that of the crystal structure (right, in gray), and Monomer I (left) is colored in gray (RMSD: 0.52 Å)

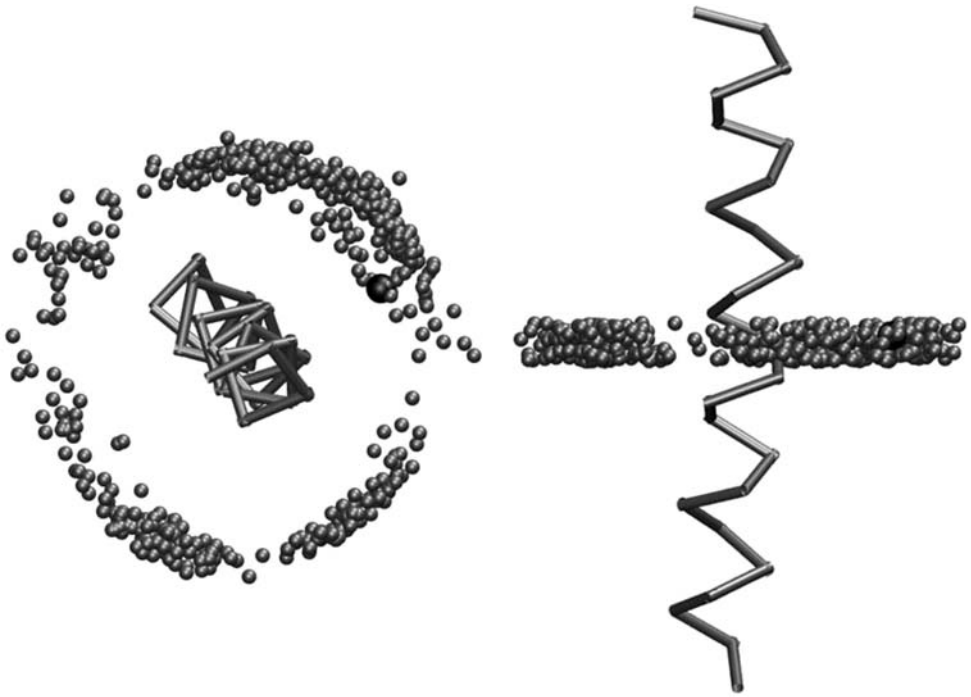

Fig. 6 The center of mass distribution of Monomer II around Monomer I of GPA from adapted 2D-BD simulations (left: top view; right: side view)

used the same protocol as described above to rank complexes. However, only 529 complexes (Fig. 6) with interaction energies smaller than −35 kcal/mol were selected for following local minimization and statistical cluster analysis.

The RMSD of α carbon atoms between the predicted and experimental structure of monomer II were calculated, and the plot of interaction energies vs. RMSD was shown in Fig. 7 (Fig. 7a, b present the results before and after local energy minimization, respectively). From Fig. 7 one can see that after local energy minimizations the lowest interaction energy complexes with the smallest RMSD to the experimental structure.

We also performed the BD stimulations without the vdw terms. About 646 complexes with negative interaction energies smaller than −12 kcal/mol were obtained from the simulations. The plot of interaction energies vs. RMSD (Fig. 7c) shows no correlations between RMSD and interaction energies. However, after we performed additional local energy minimizations with the vdw terms on these complexes, again the correlations between the interaction energy and RMSD were recovered (Fig. 3d).

A statistical cluster analysis for 529 optimized complex structures from the BD simulations with vdw terms based on 3.5 Å cutoff for all the α carbon atoms, produced 40

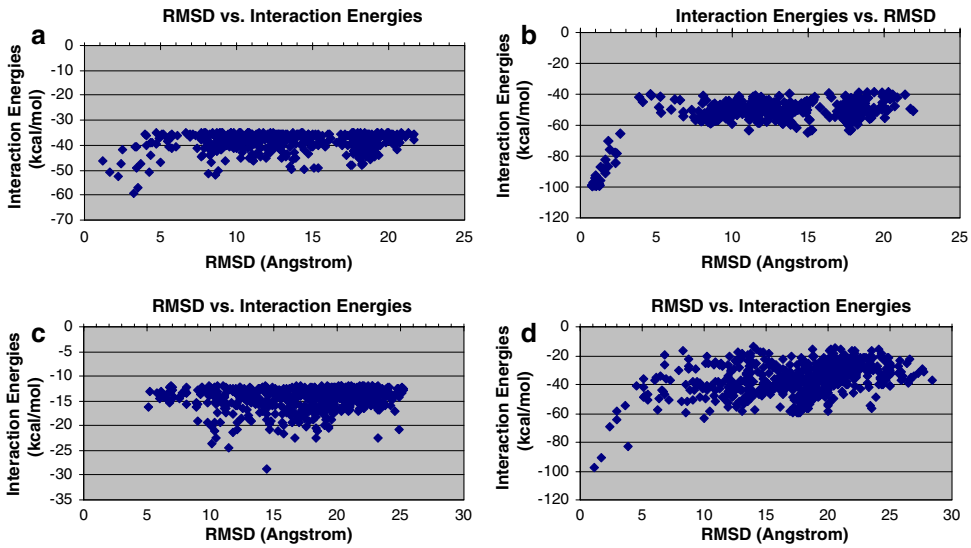

Fig. 7 Interaction energies of predicted dimer complexes vs. RMSD between the predicted and crystal structure of Monomer II of GPA. (**a**) BD simulations with vdw terms; (**b**) BD simulations with vdw terms followed by local energy minimizations; (**c**) BD simulations without vdw terms; (**d**) BD simulations without vdw terms followed by local energy minimizations

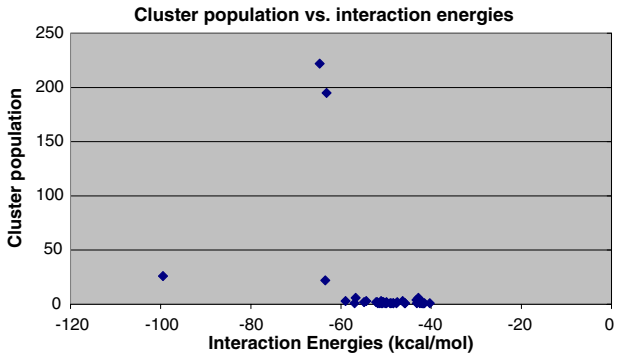

Fig. 8 Cluster population vs. lowest interaction energies between Monomers I and II of GPA in the cluster (3.5 Å cutoff based on all the α carbon atoms of Monomer II)

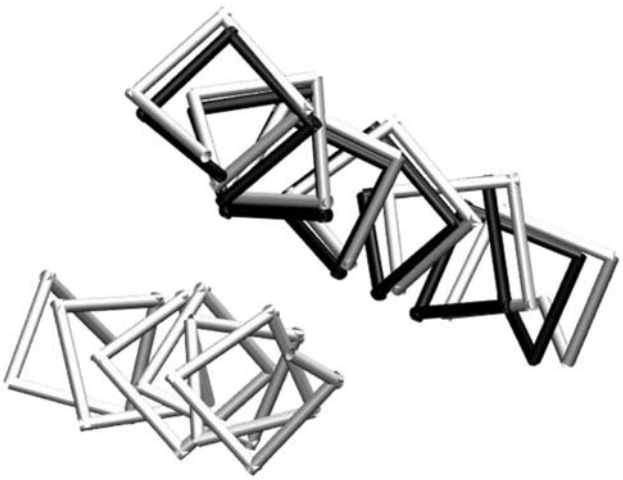

Fig. 9 Comparison of NMR (10th) and 2D-BD predicted structures of GPA. The BD-predicted Monomer II (top, in black) is very close to that of the NMR structure (top, in gray), and Monomer I (bottom) is colored in gray (RMSD: 0.78 Å)

clusters. The plot of cluster population vs. lowest interaction energies of the cluster is shown in Fig. 8. Again, the lowest energy cluster is much stable than the rest clusters. The predicted structure with lowest interaction energy superimposed on the experimental structure is shown in Fig. 9. The BD predicted structure is very close to the experimental structure (RMSD = 0.78 Å) of GPA, which again indicates success of the prediction.

Conclusions

To explore whether Brownian Dynamics simulations could predict dimerization of membrane proteins, we modified the BD program MacroDox 3.2.2 to include a van der Waals term in the interaction energy as an essential contribution to drive dimerization of membrane proteins. The adaptation of MacroDox includes: 1. Generating the membrane–water hybrid electrostatic potential maps to mimic the specific environment of membrane proteins for electrostatic interaction calculations; 2. Addition of a smoothed van der Waals potential term into the force field of the BD program for short-term van der Waals interactions; 3. Reduction of the BD sampling space from three dimensions to two dimensions to increase sampling efficiency for membrane proteins: the translations and rotations are restricted within the 2D membrane. We also implemented an RMSD-based clustering to analyze the results and to identify the cluster with the most favorable interaction energies between the two monomers. The dimer complex identified by the cluster analysis of the 2D-BD results was further refined by energy minimization to identify the most favorable local configuration. The predicted structure of the dimer of OMPLA, and GPA membrane proteins agreed with the experimental structures with a RMSD of 0.52 Å and 0.78 Å for Monomers II, respectively, which were the only monomers allowed to move during the BD simulations. The interaction energy decomposition shows that the van der Waals interactions between the two dimers are the main components for the total interaction energies for OMPLA (vdw: −307.0 kcal/mol, Elec: 5.4 kcal/mol) and GPA (vdw: −97.3 kcal/mol, Elec: −2.1 kcal/mol). The inclusion of short-range van der Waals interactions played an important role in the dimerization of OMPLA and GPA. The consistency between predicted dimer of OMPLA and GPA with the experimental structures indicates that the extended BD program could be used for prediction of dimerization of other membrane proteins, such as GPCRs.

Acknowledgements We thank Professor S. H. Northrup for his permission to adapt the MacroDox3.2.2 Program, and for his helpful discussions. We gratefully acknowledge financial support from National Institute Health Grant DC007721 (M.C.), and DC006696 (Marianna Max). The computations were made possible by grants of the National Center for Supercomputing Applications under MCB060020P and MCB070095T (MC).

References

1. Heldin CH (1995) Cell 80(2):213
2. Rios CD, Jordan BA, Gomes I, Devi LA (2001) Pharmacol Ther 92(2–3):71
3. Milligan G (2001) J Cell Sci 114(Pt 7):265
4. Angers S, Salahpour A, Bouvier M (2002) Annu Rev Pharmacol Toxicol 42:409
5. Bouvier M (2001) Nat Rev Neurosci 2(4):274
6. George SR, O'Dowd BF, Lee SP (2002) Nat Rev Drug Discov 1(10):808
7. Breitwieser GE (2004) Circ Res 94(1):17
8. Milligan G (2006) Drug Discov Today 11(11–12):541
9. Angers S, Salahpour A, Joly E, Hilairet S, Chelsky D, Dennis M, Bouvier M (2000) Proc Natl Acad Sci USA 97(7):3684
10. Dinger MC, Bader JE, Kobor AD, Kretzschmar AK, Beck-Sickinger AG (2003) J Biol Chem 278(12):10562

11. McVey M, Ramsay D, Kellett E, Rees S, Wilson S, Pope AJ, Milligan G (2001) J Biol Chem 276(17):14092
12. Fotiadis D, Liang Y, Filipek S, Saperstein DA, Engel A, Palczewski K (2003) Nature 421(6919):127
13. Liang Y, Fotiadis D, Filipek S, Saperstein DA, Palczewski K, Engel A (2003) J Biol Chem 278(24):21655
14. Fotiadis D, Liang Y, Filipek S, Saperstein DA, Engel A, Palczewski K (2004) FEBS Lett 564(3):281
15. Cheng ZJ, Miller LJ (2001) J Biol Chem 276(51):48040
16. Kota P, Reeves PJ, Rajbhandary UL, Khorana HG (2006) Proc Natl Acad Sci USA 103(9):3054
17. Davies A, Schertler GF, Gowen BE, Saibil HR (1996) J Struct Biol 117(1):36
18. Schertler GF, Hargrave PA (1995) Proc Natl Acad Sci USA 92(25):11578
19. Davies A, Gowen BE, Krebs AM, Schertler GF, Saibil HR (2001) J Mol Biol 314(3):455
20. Guo W, Shi L, Filizola M, Weinstein H, Javitch JA (2005) Proc Natl Acad Sci USA 102(48):17495
21. Filizola M, Weinstein H (2005) Febs J 272(12):2926
22. Filizola M, Weinstein H (2002) Biopolymers 66(5):317
23. Filizola M, Olmea O, Weinstein H (2002) Protein Eng 15(11):881
24. Smith GR, Sternberg MJ (2002) Curr Opin Struct Biol 12(1):28
25. Ouporov IV, Knull HR, Thomasson KA (1999) Biophys J 76(1 Pt 1):17
26. Pearson DC Jr, Gross EL (1998) Biophys J 75(6):2698
27. Lowe SL, Adrian C, Ouporov IV, Waingeh VF, Thomasson KA (2003) Biopolymers 70(4):456
28. Cui M, Shen J, Briggs JM, Luo X, Tan X, Jiang H, Chen K, Ji R (2001) Biophys J 80(4):1659
29. Cui M, Shen J, Briggs JM, Fu W, Wu J, Zhang Y, Luo X, Chi Z, Ji R, Jiang H, Chen K (2002) J Mol Biol 318(2):417
30. Fu W, Cui M, Briggs JM, Huang X, Xiong B, Zhang Y, Luo X, Shen J, Ji R, Jiang H, Chen K (2002) Biophys J 83(5):2370
31. Huang X, Liu H, Cui M, Fu W, Yu K, Chen K, Luo X, Shen J, Jiang H (2004) Curr Pharm Des 10(9):1057
32. Berman HM, Westbrook J, Feng Z, Gilliland G, Bhat TN, Weissig H, Shindyalov IN, Bourne PE (2000) Nucleic Acids Res 28(1):235
33. Snijder HJ, Ubarretxena-Belandia I, Blaauw M, Kalk KH, Verheij HM, Egmond MR, Dekker N, Dijkstra BW (1999) Nature 401(6754):717
34. Fiser A, Sali A (2003) Bioinformatics 19(18):2500
35. Fiser A, Do RK, Sali A (2000) Protein Sci 9(9):1753
36. MacKenzie KR, Prestegard JH, Engelman DM (1997) Science 276(5309):131
37. Northrup SH, Laughner T, Stevenson G (1999) MacroDox macromolecular simulation program. Tennessee Technological University, Department of Chemistry, Cookeville, TN
38. Northrup SH, Boles JO, Reynolds JCL (1987) J Phys Chem 91:5991
39. Northrup SH, Thomasson KA, Miller CM, Barker PD, Eltis LD, Guillemette JG, Inglis SC, Mauk AG (1993) Biochemistry 32(26):6613
40. Smoluchowski MV (1917) Z Phys Chem 92:129
41. Ermak DL, McCammon JA (1978) J Chem Phys 69:1352
42. Warwicker J, Watson HC (1982) J Mol Biol 157(4):671
43. Gabdoulline RR, Wade RC (1998) Methods 14(3):329
44. Nelder JA, Mead R (1965) Comput J 7:308
45. Landolt-Marticorena C, Williams KA, Deber CM, Reithmeier RA (1993) J Mol Biol 229(3):602
46. Arkin IT, Brunger AT (1998) Biochim Biophys Acta 1429(1):113
47. Killian JA, von Heijne G (2000) Trends Biochem Sci 25(9):429
48. Morris GM, Goodsell DS, Halliday RS, Huey R, Hart WE, Belew RK, Olson AJ (1998) J Comput Chem 19:1639